JOURNAL OF AGRICULTURAL AND FOOD CHEMISTRY
ARTICLE

J. Agric. Food Chem. 2010, 58, 3159–3166 3159
DOI:10.1021/jf9037419

Vinylcatechin Dimers Are Much Better Copigments for Anthocyanins than Catechin Dimer Procyanidin B3

Luís Cruz,[†] Natércia F. Brás,[‡] Natércia Teixeira,[†] Nuno Mateus,[†] Maria João Ramos,[‡] Olivier Dangles,[§] and Victor De Freitas*,[†]

[†]Centro de Investigação em Química, Departamento de Química, Faculdade de Ciências, Universidade do Porto, Rua do Campo Alegre 687, 4169-007 Porto, Portugal, [‡]REQUIMTE, Departamento de Química, Faculdade de Ciências, Universidade do Porto, Rua do Campo Alegre 687, 4169-007 Porto, Portugal, and [§]Université d'Avignon et des Pays de Vaucluse, INRA, UMR408, F-84000 Avignon, France

The binding constants (K) for the interaction of three copigments (CP), two epimeric vinylcatechin dimers (CP1 and CP2), and catechin dimer B3 (CP3) with two pigments, malvidin-3-glucoside (oenin) and malvidin-3,5-diglucoside (malvin), were determined. The K values clearly show that both vinylcatechin dimers have much higher affinity for oenin and malvin than dimer B3: $K_{CP2} > K_{CP1} \gg K_{CP3}$. Quantum mechanics and molecular dynamics calculations were also performed to interpret the binding data and specify the relative arrangement of the pigment and copigment molecules within the complexes.

KEYWORDS: Anthocyanin; vinylcatechin; procyanidin B3; copigment; copigmentation; binding constant; red wine

INTRODUCTION

Anthocyanins belong to a large family of flavonoids extensively widespread in plants. These natural pigments are responsible for the color of many flowers, fruits, and beverages such as young red wines. However, they are very unstable and susceptible to transformations in food matrices. The color displayed by anthocyanins in solution is pH-dependent. Thus, their red flavylium cation, predominant only in acidic media (pH <2), is in equilibrium with other forms at higher pH. Water addition on flavylium ions gives rise to colorless hemiketals and minor amounts of yellow chalcones, whereas proton transfer reactions lead to the formation of purple neutral quinonoid bases and the respective blue anions (*1*). Because anthocyanins have pK_h values between 2 and 3, in red wines (pH 3.2−4.0) they are expected to be present largely as colorless hemiketals ($>70\%$) (*2*). Nevertheless, these pigments are found to occur in nature mainly as flavylium cations and quinonoid bases as a result of various color-stabilizing mechanisms, such as metal complexation and the noncovalent binding of anthocyanins with themselves (self-association) or with colorless polyphenols acting as copigments (copigmentation) (*3*−*9*). The copigmentation phenomenon consists essentially in van der Waals interactions (vertical $\pi-\pi$ stacking) between the planar polarizable nuclei of the anthocyanin and the copigment. The anthocyanin−copigment complexes adopt a sandwich-like structure that stabilizes the flavylium cation chromophore (benzopyrylium) and partially protects it from the nucleophilic attack of water, thus preventing color loss (*10*−*12*). Usually, this kind of molecular association produces an increase in absorbance (hyperchromic effect) and a positive shift of the wavelength of the visible absorption maximum (bathochromic effect). The intensity of the copigmentation effect is strongly affected by many factors including the concentrations of anthocyanin and copigment, their chemical structures, the pH of the medium, the solvent, temperature, and ionic strength (*13*−*16*).

Red wine color evolution during aging is a complex process that is attributed to copigmentation phenomena (*17*−*19*) and to the progressive conversion of the original anthocyanins into new, more stable pigments. Reactions of anthocyanins with flavan-3-ols (catechins and procyanidins), either directly (*20*, *21*) or mediated by acetaldehyde (*22*, *23*), and with small molecules present in wines, namely, acetaldehyde (vitisin B) (*24*), acetoacetic acid (*25*), pyruvic acid (vitisin A) (*26*−*28*), vinylphenols (*29*−*34*), and vinylcatechin (*35*) giving rise to different families of wine pigments have been described. More recently, vinylcatechin, which is appointed in the literature as the key intermediate in the formation of pyranoanthocyanin−flavanol and vinylpyranoanthocyanin−flavanol (portisins) pigments (*36*−*41*), was shown to be unstable in an acidic model solution affording two stable diastereoisomeric vinylcatechin dimers, which were isolated and structurally characterized (*42*).

The aim of this work was to study the ability of the two vinylcatechin dimers and the common catechin dimer procyanidin B3 to act as copigments of malvidin-3-glucoside (oenin, the main grape anthocyanin) and malvidin-3,5-diglucoside (malvin) and to determine their respective copigmentation binding constants.

MATERIALS AND METHODS

Samples. Malvidin-3-glucoside (oenin chloride) was isolated from a young red table wine (*Vitis vinifera* L. cv. Touriga Nacional) by semipreparative HPLC using a reversed-phase C18 column (250 mm × 4.6 mm i.d.),

*Author to whom correspondence should be addressed (e-mail vfreitas@fc.up.pt; fax +351.226082959; telephone +351.226082862).

Published on Web 02/04/2010

as reported elsewhere (*43*). Malvidin-3,5-diglucoside (malvin chloride) was purchased from Extrasynthese (Lyon, France). Procyanidin B3 was obtained by hemisynthesis (*44*). Vinylcatechin dimers were synthesized and purified according to the procedures described in the literature (*42*). Briefly, 8-vinylcatechin (1.5 mM), previously synthesized (*45*), was incubated in a solution of 20% EtOH/H_2O at pH 2 and 30 °C. After 2 h, the vinylcatechin dimers were purified by TSK Toyopearl gel HW-40 (S) column chromatography (250 mm × 16 mm i.d.).

Copigmentation. All solutions used were prepared in a citrate buffer solution (0.2 M) at pH 3.5, and the ionic strength was adjusted to 0.5 M by the addition of sodium chloride. Each pigment/copigment solution was prepared by mixing a volume of pigment (10^{-4} M) solution with an aliquot of copigment solution to give the required pigment/copigment molar ratio of 1:0, 1:1, 1:5, 1:10, 1:20, 1:30, 1:40. Each experiment was performed in triplicate. All of the solutions were left to equilibrate for 30 min before spectroscopic measurements. For malvin, the absorbance values were collected at the wavelength (λ_I 533, 536, and 522 nm for CP1, CP2, and CP3, respectively) of the isosbestic point of the flavylium cation (10^{-4} M) and its copigmentation complexes (malvin/copigments molar ratio = 1:40). This parameter was determined in strongly acidic solutions (1 M aqueous HCl, pH ≈0) in which the flavylium ion is the sole anthocyanin form. For oenin, the absorbance values were collected at the maximum absorption wavelength of free oenin at pH 3.5 (λ_{max} 522 nm for CP1, CP2, and CP3).

UV−Visible Spectroscopy. UV−visible spectra were recorded on a Bio-Tek Power Wave XS spectrophotometer at a constant temperature of 25 °C from 360 to 830 nm (1 nm sampling interval) using a 1 cm path length cell.

Molecular Dynamics Simulations. The initial geometries of both pigments, oenin and malvin, as well as all pigment−copigment complexes, were built with the GaussView (*46*) software. To calculate the optimized geometries and electronic properties, later to be used in the parametrization of these compounds, the Gaussian 03 suite of programs (*47*) was used to perform restricted Hartree−Fock calculations (RHF), with the 6-31G(d) basis set. This methodology was chosen for its consistency with that adopted for the parametrization process in Amber8 (*48*). Atomic charges were further recalculated using RESP (*49*). Molecular dynamics simulations were performed for each isomer with the parametrization adopted in Amber, using the GAFF force field, the general Amber force field for small organic molecules. In these simulations, an explicit solvation model with pre-equilibrated TIP3P water molecules was used, filling a truncated octahedral box with a minimum 12 Å distance between the box faces and any atom of the compound. Each structure was minimized in two stages. In the first stage, the compounds were kept fixed, and only the position of the water molecules was minimized. In the second stage, the full system was minimized. Subsequently, using the Langevin temperature equilibration scheme (*50*) (at constant volume with periodic boundaries), a 100 ps MD equilibration followed by a 10 ns production run was performed for each isomer.

All simulations presented in this work were carried out using the Sander module, implemented in the Amber8 simulations package, with the Cornell force field (*51*). Bond lengths involving hydrogen atoms were constrained using the SHAKE algorithm (*52*), and the equations of motion were integrated with a 2 fs time step using the Verlet leapfrog algorithm. The nonbonding interactions were truncated with a 12 Å cutoff. The temperature of the systems was maintained at 303.15 K (*50*).

The radial distribution function (RDF), $g(r)$, describes how the atomic density varies as a function of the distance from a particular point. It gives the probability of finding a particle in the distance r from another particle. It is therefore a useful tool to describe the average structure of disordered systems, particularly of liquids (*53*). The RDF of water molecules around the reactive C2 and C4 atoms of both pigments was computed using the ptraj tool present in Amber 8.

The energies of the average minimized geometries of each complex were calculated in vacuo with the density functional theory approach, at the unrestricted B3LYP hybrid density functional level (Becke−Slater−HF exchange with Lee−Yang−Parr correlation functional) using the 6-31G-(d) basis set as implemented in the Gaussian 03 package. The optimized structures were confirmed as true minima by vibrational analysis performed at the same level of calculation. A scaling factor of 0.9804 and a temperature of 298.150 K were used for vibrational frequency and thermal energy correction calculations.

Calculation of Binding Free Energies. The MM_PBSA script (Molecular Mechanics − Poisson−Boltzmann Surface Area) (*54*) implemented in Amber 8 (*55*) was used to calculate the binding free energies for all complexes. The binding free energy was calculated using the following thermodynamic equation: $\Delta\Delta G_{binding} = \Delta G_{binding}$ (CP) − $\Delta G_{binding}$ (CP2). In each calculation, 300 snapshots of the complexes were extracted every 100 steps for the last 6000 ps of the run. The internal energy (depending on bond lengths, valence, and dihedral angles) as well as the electrostatic and van der Waals interactions was calculated using the Cornell force field (*51*) with no cutoff. The electrostatic solvation free energy was calculated by solving the Poisson−Boltzmann equation with the software Delphi v.4 (*56*, *57*). The nonpolar contribution to the solvation free energy due to van der Waals interactions between the solute and the solvent and cavity formation was modeled as a term that is dependent on the solvent-accessible surface area of the molecule. The value of the external dielectric constant used was 80.0. The value of the interior dielectric constant was set to 15. Taking into account the lack of experimental values for these compounds, we have used a value close to the dielectric constant of phenol because these molecules possess similar groups (*58*). The entropy term was not calculated because it was assumed that its contribution to $\Delta\Delta G_{binding}$ is mainly canceled by the hydrophobic effect and becomes negligible (*59*).

RESULTS AND DISCUSSION

The binding of oenin and malvin with the three copigments selected (**Figure 1**) was quantitatively evaluated through the determination of the copigmentation binding constants (K) for each pigment−copigment pair.

Interaction of Oenin with Vinylcatechin Dimers and Procyanidin B3. The copigmentation binding constants (K) for oenin (malvidin-3-*O*-β-D-glucoside) with the three copigments were estimated from a general mathematical treatment that takes into account the thermodynamics of water addition onto the flavylium ion ($pK_h = 2.70 \pm 0.01$) (*60*, *61*):

$$\frac{A_0}{A - A_0} = \frac{a}{r - a} + \frac{1}{(r - a)K} \times \frac{1}{CP_t} \quad (1)$$

Equation **1** was used for the evaluation of K, assuming a 1:1 stoichiometry for the complex and no complexation between the copigment and the colorless forms. A and A_0 stand for the visible absorbance of the pigment in the presence and absence of copigment, respectively, and CP_t represents the total copigment concentration. Parameter r is the ratio of the molar absorption coefficient of the complex to that of the free flavylium ion. Finally, one has

$$a = \frac{1}{1 + K_h 10^{pH}}$$

so that $a = 0.14$ at pH 3.5 ($pK_h = 2.70$). Thus, a plot of $A_0/(A - A_0)$ as a function of $1/CP_t$ is linear with a slope of $1/(r - a)K$ and an intercept of $a/(r - a)$. The intercept/slope ratio is aK from which K is readily obtained. The absorbance values obtained for the oenin−copigment complexes at the maximum absorption wavelength of free oenin at pH 3.5 (λ_{max} 522 nm) are presented in **Table 1**. The absorbance increase with the copigment concentration reflects the preferential binding of the copigment to the flavylium ion and the subsequent shift of the hydration equilibrium toward the colored forms. The $A_0/(A - A_0)$ versus $1/CP_t$ plot for the interaction of oenin with the three copigments gave straight lines with good correlation coefficients. The K values as well as their standard deviations are presented in **Table 2**. Vinylcatechin dimers come up as much better copigments of the grape anthocyanin oenin than procyanidin B3 (CP3). Remarkably, CP2 binds oenin ca. 3 times more strongly than its epimer CP1. The K values obtained with the two vinylcatechin dimers are also much higher than the value of 89 M^{-1} estimated for the oenin−catechin pair in the same conditions (*61*). In fact, vinylcatechin dimers bind oenin with an affinity that is comparable to that of the best natural

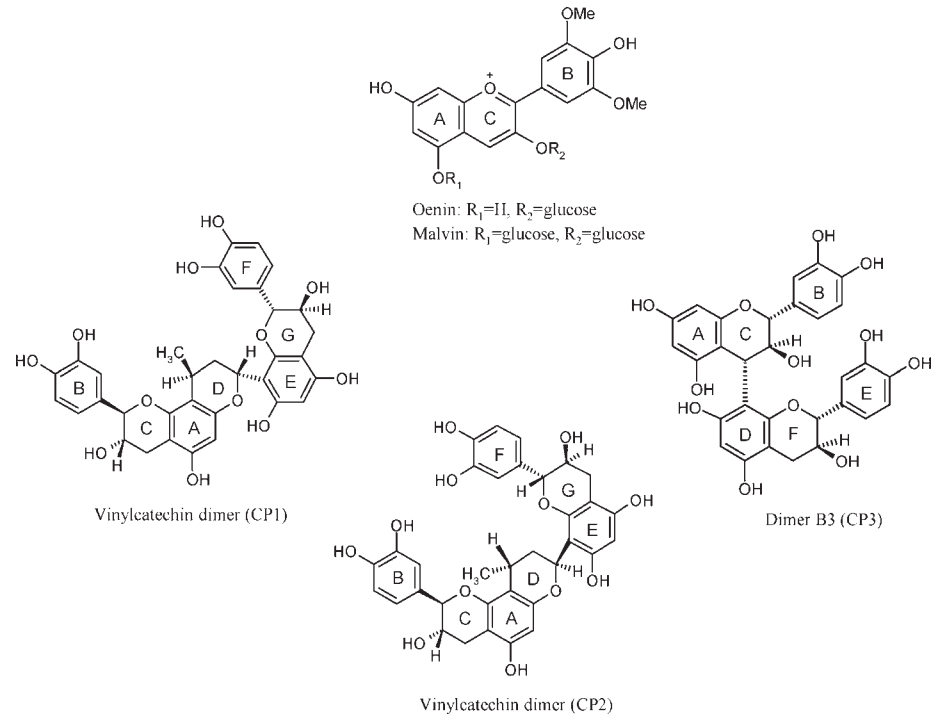

Figure 1. Chemical structures of pigments and copigments.

Table 1. Absorbance Values for the Oenin− and Malvin−Copigment Complexes

	oenin (10^{-4} M)			malvin (10^{-4} M)		
pigment/copigment molar ratio	CP1 (λ_{max} 522 nm)	CP2 (λ_{max} 522 nm)	CP3 (λ_{max} 522 nm)	CP1 (λ_{max} 533 nm)	CP2 (λ_{max} 536 nm)	CP3 (λ_{max} 522 nm)
1:0	0.308	0.295	0.302	0.150	0.142	0.154
1:1	0.324	0.339	0.305	0.161	0.166	0.155
1:5	0.412	0.460	0.314	0.228	0.258	0.164
1:10	0.491	0.543	0.323	0.286	0.350	0.163
1:20	0.610	0.650	0.350	0.457	0.520	0.178
1:30	0.698	0.706	0.367	0.569	0.651	0.204
1:40	0.786	0.753	0.391	0.617	0.671	0.224

Table 2. Binding Constants for the Oenin− and Malvin−Copigment Complexes[a]

	oenin		malvin		
copigment	K (M^{-1})	R^2	n	K (M^{-1})	R^2
CP1	1927 (±245)	0.999	1.08 (±0.04)	919 (±130)	0.995
CP2	5417 (±75)	0.998	0.90 (±0.02)	1456 (±205)	0.998
CP3	351 (±186)	0.994	1.14 (±0.08)	71 (±21)	0.985

[a] Values in parentheses are the standard deviations of the curve-fitting procedure.

copigments, which belong to the flavonol class, such as quercetin 3-rutinoside (K = 4000 M^{-1}) and quercetin mono- and disulfate (K = 14470 and 8940 M^{-1}, respectively) (*62*−*64*).

Interaction of Malvin with Vinylcatechin Dimers and Procyanidin B3. To determine the copigmentation binding constants (K) of malvin (malvidin-3,5-di-*O*-*β*-D-glucoside) with the three copigments, the simple eq **2** established by Brouillard et al. (*63*) could be applied.

$$\frac{A-A_0}{A_0} = KrCP_t^n \qquad (2)$$

Equation **2** assumes that the colored forms of the anthocyanin are negligible with respect to the colorless forms at the pH investigated, which is true for malvin but not for oenin. Indeed, at pH 3.5, the flavylium ion of malvin (pK_h = 1.52 ± 0.02) (*65*) represents no more than ca. 1% of the total pigment concentration. By contrast, oenin (pK_h = 2.70 ± 0.01) (*60*) is typically much less prone to water addition. The plot of $\ln[A - A_0)/A_0]$ as a function of ln CP_t at a suitable wavelength in the visible range should be linear with a slope identical to the stoichiometry of the complex (n, number of copigment molecules bound to the flavylium nucleus) and an intercept corresponding to ln(Kr). Because parameter r is the ratio of the molar absorption coefficient of the copigmentation complex to that of the free flavylium ion, at the isosbestic point (determined at pH ≈0 to ensure total conversion of the pigment into the flavylium form, λ_I = 533 and 536 nm for copigments 1 and 2, respectively), r = 1 by definition. Surprisingly, it was not possible to determine the isosbestic point with procyanidin B3 (CP3). Indeed, at pH ≈0, an unexpected hyperchromic effect of the flavylium−B3 complex was observed instead of a bathochromic shift typical of the copigmentation phenomena. In this case, the maximum absorption wavelength of the complex (522 nm) was selected for the calculation and parameter r was estimated to be 1.2. The absorbance values obtained for the malvin−copigment complexes for each molar ratio are presented in **Table 1**. With the three copigments, the ln $[A - A_0)/A_0]$ versus ln(CP_t) plots gave straight lines with good correlation coefficients. The slopes were found near the unit (**Table 2**), which means that the flavylium−copigment has a 1:1 stoichiometry as already reported in the literature (*12*). Assuming n = 1 for the malvin−copigment complexes, the mean K values

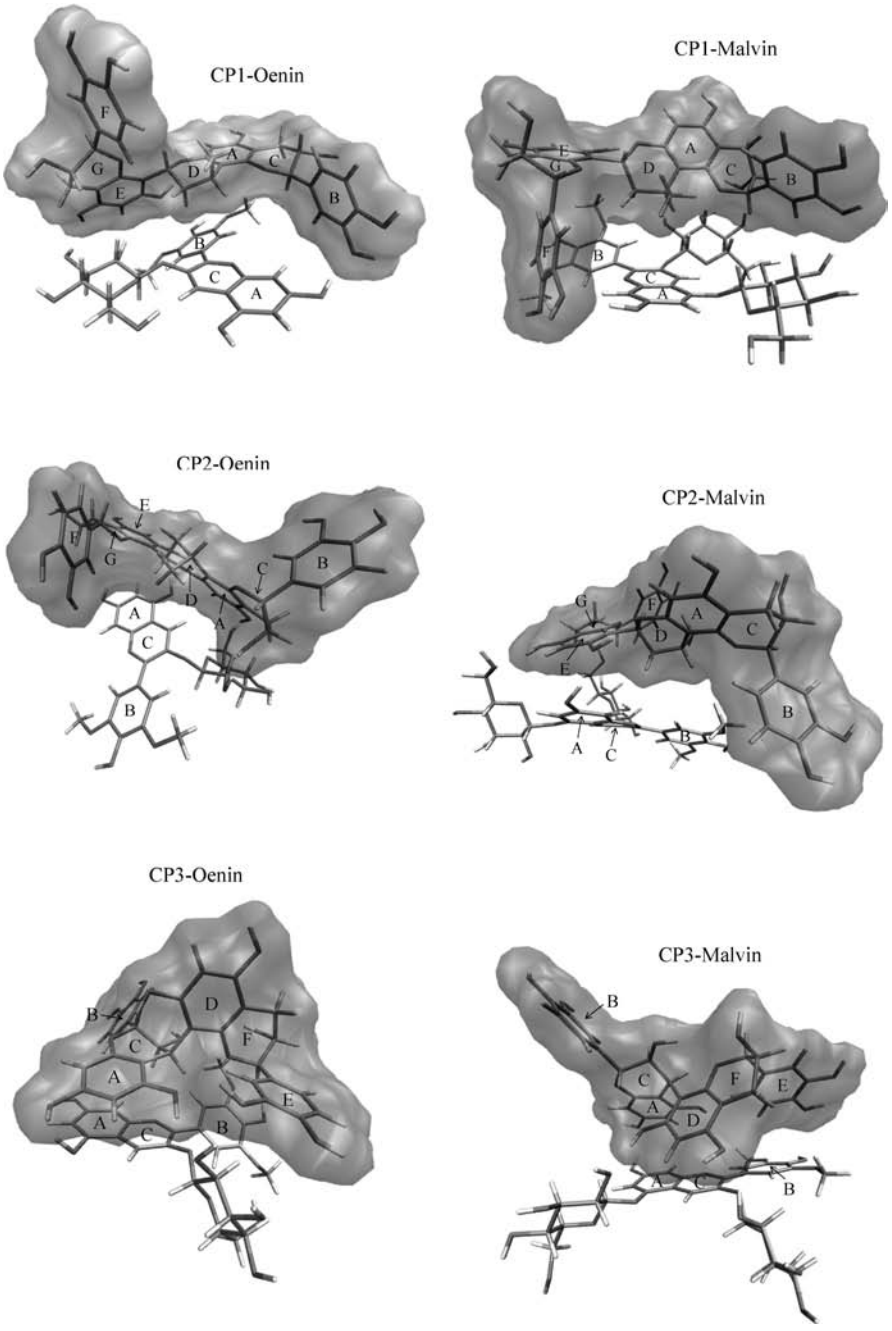

Figure 2. Optimized geometries of the copigmentation complexes. Copigment structures are represented with surfaces.

were estimated from the equation

$$\frac{A - A_0}{A_0 \mathrm{CP_t}} = Kr$$

($r = 1$ at the isosbestic point for CP1 and CP2 and $r = 1.2$ for CP3) for each copigment concentration as well as their standard deviations (**Table 2**). The binding constants obtained for both vinylcatechin dimers (CP1 and CP2) are much higher than that for dimer B3 (CP3) following the same order as in the case of oenin ($K_{CP2} > K_{CP1} > K_{CP3}$). Once again, this means that the ability of the two vinylcatechin dimers to act as malvin copigments is stronger than for dimer B3. As for the two epimers, CP2 has an affinity for malvin that is 2 times higher than that of CP1. The value of the copigmentation binding constant of the malvin−B3 complex is close to, or slightly lower than, those reported in the literature for malvin and hydroxycinnamic acids (*60*, *65*, *66*). However, for a given copigment, the *K* values of oenin remain much higher than the ones of malvin. This difference could be interpreted by the steric hindrance brought about by the second glucose residue and also possibly by a stronger contribution of the minor neutral quinonoidal bases (which could bind the copigments less strongly than the flavylium ion) in the case of malvin ($pK_a = 4.25$ for oenin; 4.0 for malvin) (*1*, *67*).

Computational Studies of Copigmentation. To better understand the differences between the copigmentation binding constants for the oenin− and malvin−copigment complexes obtained experimentally, computational studies were carried out. Molecular dynamics simulations were performed for each complex, which allowed their respective conformational space to be sampled and therefore their different conformations to be identified. The last 6 ns of each MD simulation was used for the subsequent structural analysis, as well as the calculation of the binding free energies. Taking into account the same sampling time of each MD simulation, the closest geometries to the average structures for the CP1−oenin/malvin, CP2−oenin/malvin, and CP3−oenin/malvin

complexes were obtained (**Figure 2**). The differences in the binding free energy values ($\Delta\Delta G_{binding}$) between all complexes studied were obtained using the MM_PBSA approach (*54*), as well as calculated experimentally using the copigmentation binding constants (**Table 3**). It was possibly observed that the theoretical $\Delta\Delta G_{binding}$ values fit only qualitatively with the experimental values for each anthocyanin. The quantitative differences between theoretical and experimental $\Delta\Delta G_{binding}$ values could be due to the approximations related with the MM_PBSA approach. Therefore, they might arise from the fact that the interior dielectric constant of phenol group was used instead of the one for the compounds studied herein. The relative binding free energies of the copigmentation complexes show that the ones between both pigments and the CP1 and CP3 display higher binding free energy values comparatively to CP2. Therefore, CP2−oenin/malvin complexes display higher stability and their formation is thermodynamically favored when compared to the complexes with CP1 and CP3. According to the results obtained with oenin, a higher stability for both complexes involving the vinylcatechin dimers (CP1 and CP2) was confirmed, followed by the oenin−CP3 complex. Moreover, the tendency obtained for the binding free energies is CP2 > CP1 > CP3, which is in agreement with the experimental data. Analyzing the values obtained for the complexes with the malvin pigment, the same order for the binding free energies was observed (CP2 > CP1 > CP3). However, the difference between the values for CP1 and CP3 is very small, which is not confirmed experimentally.

Table 3. Relative Binding Free Energies of the Copigmentation Complexes[a]

	$\Delta\Delta G_{binding}$ (kcal/mol)	
copigment	oenin	malvin
CP1	2.32 (0.61)	4.90 (0.27)
CP2	0.00	0.00
CP3	5.69 (1.62)	5.01 (1.79)

[a] Experimental values calculated from **Table 2** using $\Delta\Delta G = RT\,\mathrm{Ln}(K_{CP2}/K_{CPx})$ are given in parentheses.

Table 4. Average Minimal Distances between Approximately Planar Surfaces of the Pigment and Copigment Molecules in the Copigmentation Complexes[a]

	average minimal distance (Å)			
complex	benzopyrylium nucleus (AC)	B ring	Glc1	Glc2
CP1−oenin	5.12 (CAD)	6.27 (CAD)	5.53 (GE)	
CP2−oenin	3.94 (GE)	4.20 (F)	4.98 (CAD)	
CP3−oenin	4.80 (AC)	5.15 (AC)	7.50 (AC)	
CP1−malvin	5.25 (F)	4.63 (B)	8.09 (F)	8.30 (F)
CP2−malvin	5.20 (GE)	6.56 (CAD)	7.76 (GE)	7.05 (GE)
CP3−malvin	5.57 (AC)	7.00 (DF)	7.10 (DF)	6.98 (AC)

[a] Copigment rings are represented on parentheses.

Formation of the pigment−copigment complexes is driven by van der Waals interactions between the large planar surfaces of the pigment and copigment molecules and the concomitant release of high-energy water molecules from the solvation shells (hydrophobic effect). The binding could also be strengthened by hydrogen bonds involving hydroxyl groups (glucose moieties and phenolic OH). Overall, the proximity between planar surfaces of

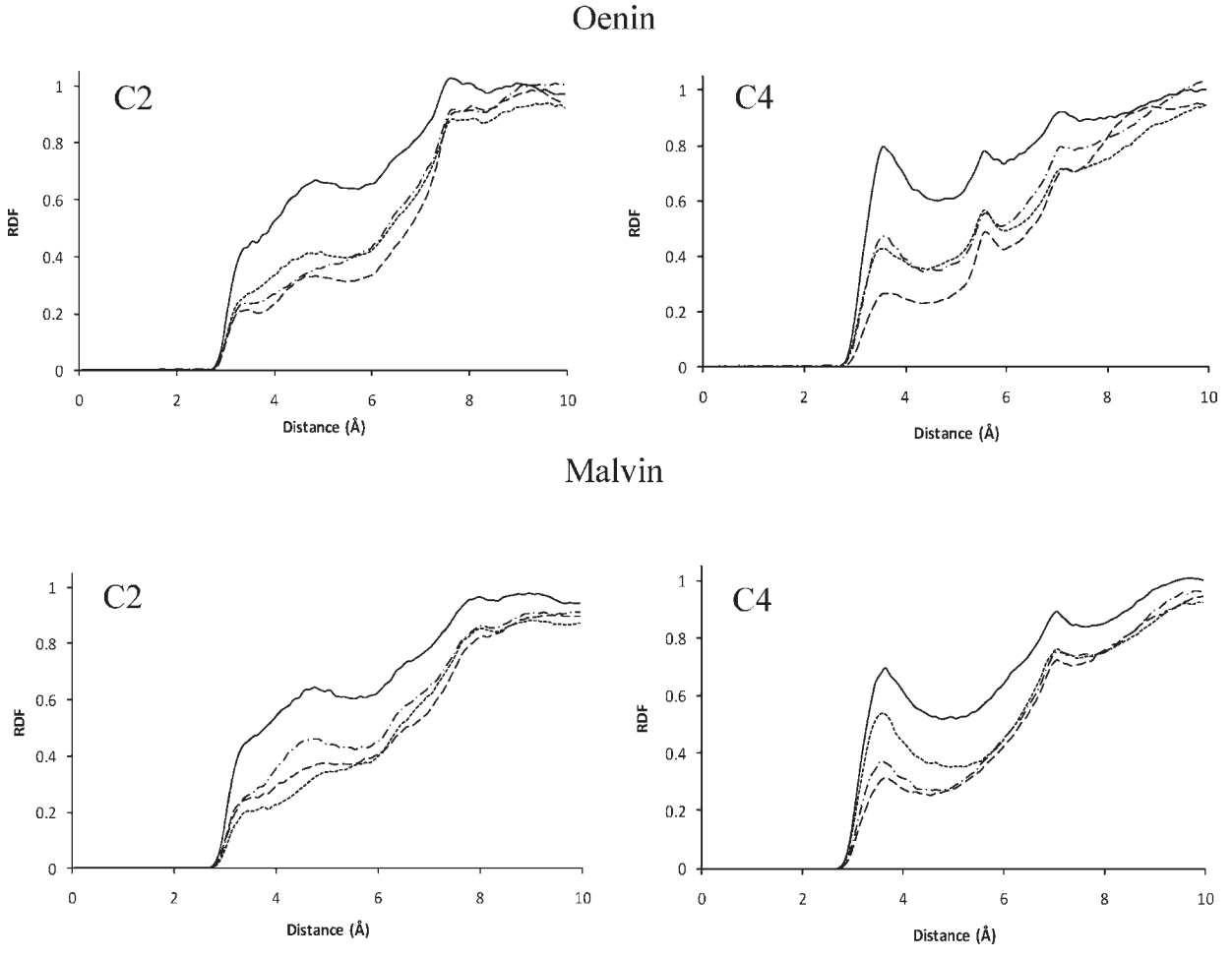

Figure 3. Radial distribution function (RDF) values for C2 and C4 atoms of oenin and malvin, in each complex studied: free oenin or malvin (—); complex with CP1 (· · ·); complex with CP2 (- -); complex with CP3 (— · —).

the pigment and copigment molecules should reflect the stability of each complex shown in **Figure 2**.

Taking this into account, the interplanar distances between all planes defined by the benzopyrylium nucleus (AC), B ring, and glucose units of the pigment and the aromatic and pyrane rings of each copigment were calculated during the last 6 ns of each MD simulation. The minimal distances thus obtained are shown in **Table 4**. Considering the average minimal distances between ring centers obtained for the oenin−copigment complexes, it was observed that the plane defined by the G and E rings of CP2 is the structural unit that is closest to the benzopyrylium ring of oenin (3.94 Å). Furthermore, the F ring and the plane defined by the A, C, and D rings of CP2 are closer to the B ring (4.20 Å) and glucose residue (4.98 Å) of oenin. Intermolecular distances of about 4 Å are consistent with van der Waals contacts. In summary, the shortest pigment−copigment distances were obtained for the oenin−CP2 complex, in agreement with its highest stability constant (*K*). Similar results were obtained with the malvin−copigment complexes, in which the same plane (G and E rings of CP2) lies at an average 5.20 Å to the benzopyrylium nucleus of malvin. The smallest average distance to the B ring of malvin was established with the B ring of CP1, whereas both glucose (Glc1 and Glc2) planes are closer to CP2 and CP3, showing similar distances for these two copigments (7.76/7.10 and 7.05/6.98 Å, respectively). Overall, these structural data show that within the complexes CP2 is closer to the pigment molecule than CP1 and CP3, which is in accordance with CP2 having the highest copigmentation binding constant for oenin and malvin.

With regard to the optimized average structures shown in **Figure 2**, it was observed that copigments 1 and 2 offer large planar surfaces for the establishment of multiple van der Waals interactions with the anthocyanin chromophore. The structural unit specific to the vinylcatechin dimers is the C−A−D tricyclic nucleus that provides a large roughly planar polarizable surface that must be prone to strong π stacking interactions. Therefore, vinylcatechin dimers should form most stable copigmentation complexes than B3 copigment. However, it was observed that the B and E nuclei in CP2 are in a cis configuration, whereas in CP1 there are in a trans configuration. Hence, CP2 provides a most accessible face for the C−A−D tricyclic nucleus, the one that is opposite to the B and E nuclei, allowing a closer contact with the benzopyrylium nucleus of the anthocyanin. This fact contributes to the best binding mode and thus to the much higher *K* values obtained for the CP2 complex.

For both oenin− and malvin−CP3 complexes, it was observed that the most favorable conformation of CP3 showed the catechin units facing opposite sides. This orientation prevents a simultaneous interaction of both catechin moieties with the flavylium nucleus, which is in agreement with CP3 having the smallest copigmentation binding constant.

Although the flavylium nucleus makes the major contribution to the copigmentation driving force, it was verified that the additional glucose residue of malvin disturbs the packing between the pigment and copigment molecules, thus lowering the *K* values.

Interactions between the flavylium ion and the copigment, either π stacking or electrostatic or both, must also provide some protection to the chromophore against the attack of water molecules at the positively charged carbons C4 and C2 (preferentially) and the subsequent formation of the colorless hemiketal, in agreement with the hyperchromic effect observed. With this in mind, the radial distribution function (RDF) of water molecules around the two reactive carbon atoms (C2 and C4) was analyzed for each pigment in their free and copigment-bound forms. The graphs presented in **Figure 3** show that in the free pigments the probability of the presence of the any water molecule increases significantly from ca. 2.8 Å. Similar (albeit lower) increments were obtained for the RDF values in all copigment-bound forms. In particular, pigment−CP2 complexes seem to show the lowest probability increment, suggesting that the pyrylium ring of the anthocyanins is less accessible to water molecules.

In conclusion, despite the two catechin units they have in common, the three copigments studied have quite different abilities to bind oenin and malvin as demonstrated by the copigmentation binding constants (*K*) calculated. The diverse spatial conformations adopted by the vinylcatechin dimers around the pigments allow multiple noncovalent interactions between relatively hydrophobic planar surfaces. The corresponding copigmentation complexes are the most stable reported so far with flavanols. Consequently, the vinylcatechin dimers could provide substantial protection to colors expressed by anthocyanins in red wine.

LITERATURE CITED

(1) Brouillard, R.; Delaporte, B. Chemistry of anthocyanin pigments. 2. Kinetic and thermodynamic study of proton-transfer, hydration, and tautomeric reactions of malvidin 3-glucoside. *J. Am. Chem. Soc.* **1977**, *99*, 8461–8468.

(2) Duenas, M.; Salas, E.; Cheynier, V.; Dangles, O.; Fulcrand, H. UV−visible spectroscopic investigation of the 8,8-methylmethine catechin-malvidin 3-glucoside pigments in aqueous solution: structural transformations and molecular complexation with chlorogenic acid. *J. Agric. Food Chem.* **2006**, *54*, 189–196.

(3) Asen, S.; Stewart, R. N.; Norris, K. H. Copigmentation of anthocyanins in plant-tissues and its effect on color. *Phytochemistry* **1972**, *11*, 1139–1144.

(4) Brouillard, R.; Dangles, O. Flavanoids and flower colour. In *The Flavonoids. Advances in Research since 1986*; Harborne, J. B., Ed.; Chapman and Hall: London, U.K., 1993; pp 565−588.

(5) Dangles, O. Anthocyanin complexation and colour expression. *Analusis* **1997**, *25*, M50–M52.

(6) Goto, T.; Kondo, T. Structure and molecular stacking of anthocyanins − flower color variation. *Angew. Chem., Int. Ed. Engl.* **1991**, *30*, 17–33.

(7) Haslam, E. *Anthocyanin Copigmentation − Fruit and Floral Pigment*; Cambridge University Press: Cambridge, U.K., 1998; pp 262−297.

(8) Robinson, G. M.; Robinson, R. A survey of anthocyanins. I. *Biochem. J.* **1931**, *25*, 1687–1705.

(9) Boulton, R. The copigmentation of anthocyanins and its role in the color of red wine: a critical review. *Am. J. Enol. Vitic.* **2001**, *52*, 67–87.

(10) Goto, T. Structure, stability and color variation of natural anthocyanins. *Prog. Chem. Org. Nat. Prod.* **1987**, *52*, 113–158.

(11) Goto, T.; Tamura, H.; Kawai, T.; Hoshino, T.; Harada, N.; Kondo, T. Chemistry of metalloanthocyanins. *Ann. N.Y. Acad. Sci.* **1986**, *471*, 155–173.

(12) Santos-Buelga, C.; De Freitas, V., Influence of phenolics on wine organoleptic properties. In *Wine Chemistry and Biochemistry*; Moreno-Arribas, M. V., Polo, M. C., Eds.; 2009; pp 529−570.

(13) Mazza, G.; Brouillard, R. The mechanism of co-pigmentation of anthocyanins in aqueous solutions. *Phytochemistry* **1990**, *29*, 1097–1102.

(14) Asen, S.; Stewart, R. N.; Norris, K. H. Co-pigmentation effect of quercetin glycosides on absorption characateristics of cyanidin glycosides and color of red wing azalea. *Phytochemistry* **1971**, *10*, 171–175.

(15) Asen, S.; Stewart, R. N.; Norris, K. H. Copigmentation of aurone and flavone from petals of *Antirrhinum-majus*. *Phytochemistry* **1972**, *11*, 2739–2741.

(16) Chen, L. J.; Hrazdina, G. Structural aspects of anthocyanin−flavonoid complex-formation and its role in plant color. *Phytochemistry* **1981**, *20*, 297–303.

(17) Brouillard, R.; Dangles, O. Anthocyanin molecular interactions: the first step in the formation of new pigments during wine aging? *Food Chem.* **1994**, *51*, 365–371.

(18) Liao, H.; Cai, Y.; Haslam, E. Polyphenols interactions. Anthocyanins: copigmentation and colour changes in red wines. *J. Sci. Food Agric.* **1992**, *59*, 299–305.
(19) Mistry, T. V.; Cai, Y.; Lilley, T. H.; Haslam, E. Polyphenol interactions. Part 5. Anthocyanin co-pigmentation. *J. Chem. Soc., Perkin Trans. 2* **1991**, 1287–1296.
(20) Remy, S.; Fulcrand, H.; Labarbe, B.; Cheynier, V.; Moutounet, M. First confirmation in red wine of products resulting from direct anthocyanin−tannin reactions. *J. Sci. Food Agric.* **2000**, *80*, 745–751.
(21) Santos-Buelga, C.; Bravo-Haro, S.; Rivas-Gonzalo, J. C. Interactions between catechin and malvidin-3-monoglucoside in model solutions. *Z. Lebensm.-Unters.-Forsch.* **1995**, 269–274.
(22) Escribano-Bailón, T.; Dangles, O.; Brouillard, R. Coupling reactions between flavylium ions and catechin. *Phytochemistry* **1996**, *41*, 1583–1592.
(23) Es-Safi, N. E.; Fulcrand, H.; Cheynier, V.; Moutounet, M. Studies on the acetaldehyde-induced condensation of (−)-epicatechin and malvidin 3-*O*-glucoside in a model solution system. *J. Agric. Food Chem.* **1999**, *47*, 2096–2102.
(24) Bakker, J.; Timberlake, C. F. Isolation, identification, and characterization of new color-stable anthocyanins occurring in some red wines. *J. Agric. Food Chem.* **1997**, *45*, 35–43.
(25) He, J.; Santos-Buelga, C.; Silva, A. M. S.; Mateus, N.; De Freitas, V. Isolation and structural characterization of new anthocyanin-derived yellow pigments in aged red wines. *J. Agric. Food Chem.* **2006**, *54*, 9598–9603.
(26) Bakker, J.; Bridle, P.; Honda, T.; Kuwano, H.; Saito, N.; Terahara, N.; Timberlake, C. F. Isolation and identification of a new anthocyanin occurring in some red wines. *Phytochemistry* **1997**, *44*, 1375–1382.
(27) Fulcrand, H.; Benabdeljalil, C.; Rigaud, J.; Cheynier, V.; Moutounet, M. A new class of wine pigments generated by reaction between pyruvic acid and grape anthocyanins. *Phytochemistry* **1998**, *47*, 1401–1407.
(28) Mateus, N.; Silva, A. M. S.; Vercauteren, J.; De Freitas, V. Occurrence of anthocyanin-derived pigments in red wines. *J. Agric. Food Chem.* **2001**, *49*, 4836–4840.
(29) Fulcrand, H.; Cameira dos Santos, P.; Sarni-Manchado, P.; Cheynier, V.; Favre-Bonvin, J. Structure of new anthocyanin-derived wine pigments. *J. Chem. Soc., Perkin Trans. 1* **1996**, 735–739.
(30) Hayasaka, Y.; Asenstorfer, R. E. Screening for potential pigments derived from anthocyanins in red wine using nano-electrospray tandem mass spectrometry. *J. Agric. Food Chem.* **2002**, *50*, 756–761.
(31) Schwarz, M.; Wabnitz, T. C.; Winterhalter, P. Pathway leading to the formation of anthocyanin−vinylphenol adducts and related pigments in red wines. *J. Agric. Food Chem.* **2003**, *51*, 3682–3687.
(32) Cameira dos Santos, P. J.; Brillouet, J. M.; Cheynier, V.; Moutounet, M. Detection and partial characterisation of new anthocyanins derived pigments in wine. *J. Sci. Food Agric.* **1996**, *70*, 204–208.
(33) Schwarz, M.; Jerz, G.; Winterhalter, P. Isolation and structure of pinotin A, a new anthocyanin derivative from Pinotage wine. *Vitis* **2003**, *42*, 105–106.
(34) Schwarz, M.; Picazo-Bacete, J. J.; Winterhalter, P.; Hermosin-Gutierrez, I. Effect of copigments and grape cultivar on the color of red wines fermented after the addition of copigments. *J. Agric. Food Chem.* **2005**, *53*, 8372–8381.
(35) Cruz, L.; Teixeira, N.; Silva, A. M. S.; Mateus, N.; Borges, J.; De Freitas, V. Role of vinylcatechin in the formation of pyrano-malvidin-3-glucoside-(+)-catechin. *J. Agric. Food Chem.* **2008**, *56*, 10980–10987.
(36) Francia-Aricha, E. M.; Guerra, M. T.; Rivas-Gonzalo, J. C.; Santos-Buelga, C. New anthocyanin pigments formed after condensation with flavanols. *J. Agric. Food Chem.* **1997**, *45*, 2262–2265.
(37) Mateus, N.; Carvalho, E.; Carvalho, A. R. F.; Melo, A.; Gonzalez-Paramas, A. M.; Santos-Buelga, C.; Silva, A. M. S.; De Freitas, V. Isolation and structural characterization of new acylated anthocyanin−vinyl−flavanol pigments occurring in aging red wines. *J. Agric. Food Chem.* **2003**, *51*, 277–282.
(38) Mateus, N.; Pascual-Teresa, S. d.; Rivas-Gonzalo, J. C.; Santos-Buelga, C.; De Freitas, V. Structural diversity of anthocyanin-derived pigments in port wines. *Food Chem.* **2002**, *76*, 335–342.
(39) Mateus, N.; Silva, A. M. S.; Rivas-Gonzalo, J. C.; Santos-Buelga, C.; De Freitas, V. A new class of blue anthocyanin-derived pigments isolated from red wines. *J. Agric. Food Chem.* **2003**, *51*, 1919–1923.
(40) Mateus, N.; Silva, A. M. S.; Santos-Buelga, C.; Rivas-Gonzalo, J. C.; De Freitas, V. Identification of anthocyanin−flavanol pigments in red wines by NMR and mass spectrometry. *J. Agric. Food Chem.* **2002**, *50*, 2110–2116.
(41) Oliveira, J.; Santos-Buelga, C.; Silva, A. M. S.; De Freitas, V.; Mateus, N. Chromatic and structural features of blue anthocyanin-derived pigments present in Port wine. *Anal. Chim. Acta* **2006**, *563*, 2–9.
(42) Cruz, L.; Brás, N. F.; Teixeira, N.; Fernandes, A.; Mateus, N.; Ramos, M. J.; Rodríguez-Borges, J.; De Freitas, V. Synthesis and structural characterization of two diasteroisomers of vinylcatechin dimers. *J. Agric. Food Chem.* **2009**, *57*, 10341–10348.
(43) Pissarra, J.; Mateus, N.; Rivas-Gonzalo, J. C.; Santos-Buelga, C.; De Freitas, V. Reaction between malvidin 3-glucoside and (+)-catechin in model solutions containing different aldehydes. *J. Food Sci.* **2003**, *68*, 476–481.
(44) Geissman, T. A.; Yoshimura, N. N. Synthetic proanthocyanidin. *Tetrahedron Lett.* **1966**, *7*, 2669–2673.
(45) Cruz, L.; Borges, E.; Silva, A. M. S.; Mateus, N.; De Freitas, V. Synthesis of a new (+)-catechin-derived compound: 8-vinylcatechin. *Org. Chem. Lett.* **2008**, *5*, 530–536.
(46) Gaussian Inc. Carnegie Office Park, Bldg. 6, Pittsburgh, PA.
(47) Frisch, M. J.; Trucks, G. W.; Schlegel, H. B.; Scuseria, G. E.; Robb, M. A.; Cheeseman, J. R.; Montgomery, J. A., Jr.; Vreven, T.; Kudin, K. N.; Burant, J. C.; Millam, J. M.; Iyengar, S. S.; Tomasi, J.; Barone, V.; Mennucci, B.; Cossi, M.; Scalmani, G.; Rega, N.; Petersson, G. A.; Nakatsuji, H.; Hada, M.; Ehara, M.; Toyota, K.; Fukuda, R.; Hasegawa, J.; Ishida, M.; Nakajima, T.; Honda, Y.; Kitao, O.; Nakai, H.; Klene, M.; Li, X.; Knox, J. E.; Hratchian, H. P.; Cross, J. B.; Bakken, V.; Adamo, C.; Jaramillo, J.; Gomperts, R.; Stratmann, R. E.; Yazyev, O.; Austin, A. J.; Cammi, R.; Pomelli, C.; Ochterski, J. W.; Ayala, P. Y.; Morokuma, K.; Voth, G. A.; Salvador, P.; Dannenberg, J. J.; Zakrzewski, V. G.; Dapprich, S.; Daniels, A. D.; Strain, M. C.; Farkas, O.; Malick, D. K.; Rabuck, A. D.; Raghavachari, K.; Foresman, J. B.; Ortiz, J. V.; Cui, Q.; Baboul, A. G.; Clifford, S.; Cioslowski, J.; Stefanov, B. B.; Liu, G.; Liashenko, A.; Piskorz, P.; Komaromi, I.; Martin, R. L.; Fox, D. J.; Keith, T.; Al-Laham, M. A.; Peng, C. Y.; Nanayakkara, A.; Challacombe, M.; Gill, P. M. W.; Johnson, B.; Chen, W.; Wong, M. W.; Gonzalez, C.; Pople, J. A. Gaussian 03 Inc., revision B.04 ed.; Pittsburgh, PA, 2003.
(48) Case, D. A.; Darden, T. A.; Cheatham, T. E., III; Simmerling, C. L.; Wang, J.; Duke, R. E.; Luo, R.; Merz, H. M.; Wang, B.; Pearlman, D. A.; Crowley, M.; Brozell, S.; Tsui, V.; Gohlke, H.; Mongan, J.; Hornak, V.; Cui, G.; Beroza, P.; Schafmeister, C.; Caldwell, J. W.; Ross, W. S.; Kollman, P. A. *AMBER 8*; University of California: San Francisco, CA, 2004.
(49) Bayly, C. I.; Cieplak, P.; Cornell, W. D.; Kollman, P. A. A well-behaved electrostatic potential based method using charge restraints for deriving atomic charges − the RESP model. *J. Phys. Chem.* **1993**, *97*, 10269–10280.
(50) Izaguirre, J. A.; Catarello, D. P.; Wozniak, J. M.; Skeel, R. D. Langevin stabilization of molecular dynamics. *J. Chem. Phys.* **2001**, *114*, 2090–2098.
(51) Cornell, W. D.; Cieplak, P.; Bayly, C. I.; Gould, I. R.; Merz, K. M.; Ferguson, D. M.; Spellmeyer, D. C.; Fox, T.; Caldwell, J. W.; Kollman, P. A. A 2nd generation force-field for the simulation of proteins, nucleic-acids, and organic-molecules. *J. Am. Chem. Soc.* **1995**, *117*, 5179–5197.
(52) Ryckaert, J. P.; Ciccotti, G.; Berendsen, H. J. C. Numerical-integration of Cartesian equations of motion of a system with constraints − molecular-dynamics of N-alkanes. *J. Comput. Phys.* **1977**, *23*, 327–341.
(53) McQuarrie, D. A. *Statistical Mechanics*; Harper Collins Publishers: New York, 1976.
(54) Kollman, P. A.; Massova, I.; Reyes, C.; Kuhn, B.; Huo, S. H.; Chong, L.; Lee, M.; Lee, T.; Duan, Y.; Wang, W.; Donini, O.;

Cieplak, P.; Srinivasan, J.; Case, D. A.; Cheatham, T. E. Calculating structures and free energies of complex molecules: combining molecular mechanics and continuum models. *Acc. Chem. Res.* **2000**, *33*, 889–897.

(55) Case, D. A.; Cheatham, T. E.; Darden, T.; Gohlke, H.; Luo, R.; Merz, K. M.; Onufriev, A.; Simmerling, C.; Wang, B.; Woods, R. J. The Amber biomolecular simulation programs. *J. Comput. Chem.* **2005**, *26*, 1668–1688.

(56) Rocchia, W.; Alexov, E.; Honig, B. In *Extending the Applicability of the Nonlinear Poisson−Boltzmann Equation: Multiple Dielectric Constants and Multivalent Ions*; *J. Phys. Chem. B* **2001**, *105*, 6507−6514.

(57) Rocchia, W.; Sridharan, S.; Nicholls, A.; Alexov, E.; Chiabrera, A.; Honig, B. Rapid grid-based construction of the molecular surface and the use of induced surface charge to calculate reaction field energies: applications to the molecular systems and geometric objects. *J. Comput. Chem.* **2002**, *23*, 128–137.

(58) Philip, J. C.; Haynes, D. CV—The dielectric constants of phenols and their ethers dissolved in benzene and *m*-xylene. *J. Chem. Soc. Trans.* **1905**, *87*, 998–1003.

(59) Huo, S.; Massova, I.; Kollman, P. A. Computational alanine scanning of the 1:1 human growth hormone-receptor complex. *J. Comput. Chem.* **2002**, *23*, 15–27.

(60) Dangles, O.; Elhajji, H. Synthesis of 3-methoxy-flavylium and 3-(β-D-glucopyranosyloxy)flavylium ions − influence of the flavylium substitution pattern on the reactivity of anthocyanins in aqueous-solution. *Helv. Chim. Acta* **1994**, *77*, 1595–1610.

(61) Malien-Aubert, C.; Dangles, O.; Amiot, M. J. Influence of procyanidins on the color stability of oenin solutions. *J. Agric. Food Chem.* **2002**, *50*, 3299–3305.

(62) Alluis, B.; Dangles, O. Quercetin (=2-(3,4-dihydroxyphenyl)-3,5,7-trihydroxy-4*H*-1-benzopyran-4-one) glycosides and sulfates: chemical synthesis, complexation, and antioxidant properties. *Helv. Chim. Acta* **2001**, *84*, 1133–1156.

(63) Brouillard, R.; Mazza, G.; Saad, Z.; Albrechtgary, A. M.; Cheminat, A. The copigmentation reaction of anthocyanins − a microprobe for the structural study of aqueous-solutions. *J. Am. Chem. Soc.* **1989**, *111*, 2604–2610.

(64) Dangles, O.; Brouillard, R. Poplyphenol interactions − the copigmentation case − thermodynamic data from temperature-variation and relaxation kinetics−medium effect. *Can. J. Chem.* **1992**, *70*, 2174–2189.

(65) Galland, S.; Mora, N.; Abert-Vian, M.; Rakotomanomana, N.; Dangles, O. Chemical synthesis of hydroxycinnamic acid glucosides and evaluation of their ability to stabilize natural colors via anthocyanin copigmentation. *J. Agric. Food Chem.* **2007**, *55*, 7573–7579.

(66) Markovic, J. M. D.; Petranovic, N. A.; Baranac, J. M. A spectrophotometric study of the copigmentation of malvin with caffeic and ferulic acids. *J. Agric. Food Chem.* **2000**, *48*, 5530–5536.

(67) Brouillard, R.; Delaporte, B.; Dubois, J. E. Chemistry of anthocyanin pigments. 3. Relaxation amplitudes in pH-jump experiments. *J. Am. Chem. Soc.* **1978**, *100*, 6202–6205.

Received for review October 27, 2009. Revised manuscript received December 17, 2009. Accepted January 22, 2010. This research was supported by the research project grants (PTDC/QUI/67681/2006) and CONC-REEQ/275/2001 funding from FCT (Fundação para a Ciência e a Tecnologia) from Portugal. L.C. and N.F.B. gratefully acknowledge Ph.D. grants from FCT (SFRH/BD/30915/2006 and SFRH/BD/31359/2006, respectively).